

## Ion-temperature measurement via laser scattering on ion Bernstein waves

G. A. Wurden, M. Ono, and K. L. Wong

*Plasma Physics Laboratory, Princeton University, Princeton, New Jersey 08544*

(Received 14 July 1982)

Hydrogen ion temperature has been measured in a warm toroidal plasma with externally launched ion Bernstein waves detected by CO<sub>2</sub> laser scattering. Radial scanning of the laser beam allows precise determination of  $k_{\perp}$  for the finite ion Larmor radius wave ( $\omega \leq 2\Omega_i$ ). Knowledge of the magnetic field strength and ion concentration then give a radially resolved ion temperature, independent of  $T_e$ . Probe measurements and Doppler broadening of Ar II 4806 Å give excellent agreement.

Coherent light scattering from plasmas has been shown to be a powerful diagnostic tool, having previously been employed to observe driven electron Bernstein waves,<sup>1</sup> driven ion acoustic waves,<sup>2-3</sup> driven lower hybrid waves,<sup>4</sup> and with a considerable degree of difficulty, the spectrum of thermal fluctuations to measure  $T_e/T_i$ .<sup>5</sup> This last measurement is generally recognized to require a pulsed, high-power (megawatt) laser of good spectral mode purity and a very sensitive broadband ( $\sim 1$  GHz) heterodyne detector for hydrogen ion temperature ( $T_i$ ) measurement in a medium density ( $10^{13} - 10^{14}$  cm<sup>-3</sup>) hot transient plasma.<sup>6</sup> Hydrogen ion temperature is a critical plasma parameter which becomes increasingly difficult to measure by conventional techniques in large fusion devices. The present paper demonstrates the first use of low power continuous-wave (cw) CO<sub>2</sub> laser scattering to detect externally launched ion Bernstein (IBW) test waves giving a nonperturbing measurement of the ion temperature in a warm, low density ( $T_i \sim 1.5$  eV,  $T_e \sim 2$  eV,  $n_e \sim 3 \times 10^{10}$  cm<sup>-3</sup>) hydrogen plasma. This method is distinctly different from previously proposed ion cyclotron techniques,<sup>7-9</sup> in that we do not require electron temperature information to obtain  $T_i$ .

The appropriate electrostatic dispersion relation for  $\omega = \sigma(\Omega_i)$  is<sup>10</sup>

$$k_{\perp}^2 K_{xx} + k_{\parallel}^2 K_{zz} = 0, \quad (1)$$

where

$$K_{xx} = 1 + \sum_{\sigma} \omega_{p\sigma}^2 \exp(-b_{\sigma}) b_{\sigma}^{-1} \sum_{n=1}^{\infty} I_n(b_{\sigma}) \frac{2n^2}{(n^2 \Omega_{\sigma}^2 - \omega^2)},$$

$$K_{zz} = 1 + 2(\omega_{pe}^2/\omega^2)y^2[1 + yZ(y)] \approx -\omega_{pe}^2/\omega^2,$$

and  $b_{\sigma} \equiv k_{\perp}^2 T_{\sigma}/m_{\sigma} \Omega_{\sigma}^2$ ,  $\sigma$  denotes species,  $I_n$  is the modified Bessel function,  $y \equiv (\omega/k_{\parallel})(m_e/2T_e)^{1/2}$ , and  $Z$  is the plasma dispersion function. Under the assumptions that  $\omega^2 \ll \omega_{pe}^2$ ,  $y \gg 1$  to avoid electron Landau damping and  $k_{\perp}/k_{\parallel} \gg (m_i/m_e)^{1/2}$  so that the second term in Eq. (1) is negligible, the perpendicular

lar wave phase velocity is, in general, proportional to the ion thermal velocity. In particular, for a single-species plasma, and  $\omega \leq 2\Omega_i$ , we have

$$\lambda_{\perp} \approx V_{Ti} f^{-1} \{3/[4(\Omega_i^2/\omega^2) - 1]\}^{1/2}, \quad (2)$$

where  $f$  is the wave frequency,  $V_{Ti} = (T_i/m_i)^{1/2}$ , having used a small argument expansion for  $I_2(b_i)$ . Equation (2) clearly shows the dependence of IBW perpendicular wavelength  $\lambda_{\perp}$  on the local ion temperature and magnetic field. We note that the electron Bernstein wave has been previously used to measure  $T_e$ .<sup>11</sup> Since the IBW is associated with ion motion in the bulk of the ion distribution function, the temperature obtained from the real part of the dispersion relation [Eq. (1)] is only weakly affected by possible fast tail components.

The experiment was performed in the steady-state ACT-1 (Advanced Concepts Torus) filament produced hydrogen plasma, of major radius  $R_0 = 59$  cm and minor radius  $r_0 = 9$  cm. A schematic of the machine geometry is shown in Fig. 1(a). H<sub>2</sub> neutral fill pressure can be lowered to an absolute  $2 \times 10^{-5}$  Torr, with a base pressure  $\sim 5 \times 10^{-7}$  Torr, resulting in a  $T_e \approx T_i \leq 2$  eV hydrogen plasma. The IBW is excited by two external ( $R = 65.5$  cm) 12-cm high  $\times$  5-cm wide vertical flat plate antennas, spaced 17 cm apart and driven 180° out of phase to define  $\lambda_{\parallel} \sim 34$  cm.<sup>12</sup>

The laser system [see Fig. 1(b)] consists of a single mode 50-W cw CO<sub>2</sub> laser at  $\lambda_0 = 10.6$  μm, used in conjunction with a liquid-helium-cooled copper-doped germanium photoconductor, configured in a small angle (3–26 mrad) forward scattering geometry.<sup>13</sup> Matched Gaussian beam waists (radius at  $1/e^2$  power point)  $a_0 \approx 3.3$  mm in the plasma give an angle defined  $k$  resolution  $\Delta k_{\perp} = 2/a_0 \approx 6$  cm<sup>-1</sup>. The system noise equivalent power in the frequency band of interest (9–13 MHz) at the fiber optic receiver is  $NEP \approx 2 \times 10^{-18}$  W/Hz, as determined by black body and gain-recombination noise measurements. Ob-

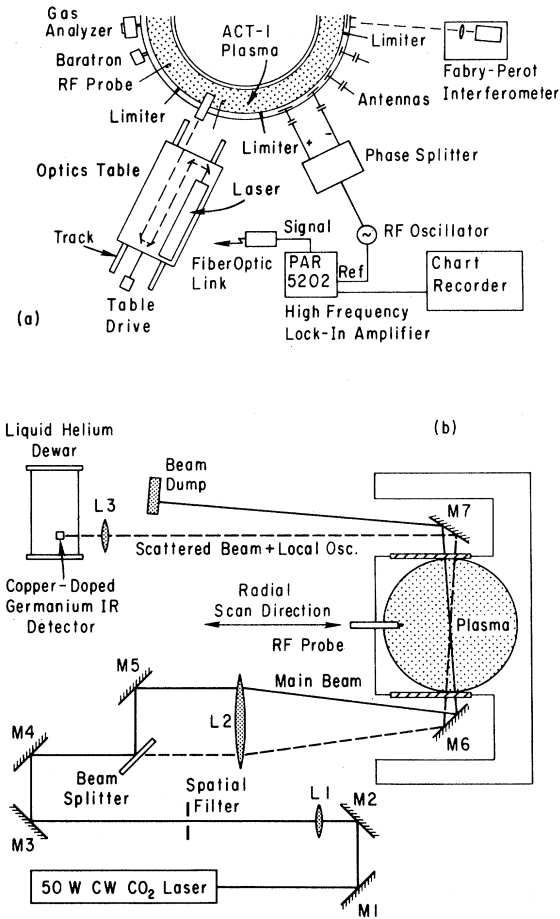


FIG. 1. (a) Schematic of the experimental apparatus. (b) Diagram of the laser scattering geometry. Mirrors  $M6$  and  $M7$  move with the optics table.

served density fluctuation levels at the pump frequency range from  $\tilde{n} \sim 5 \times 10^5$  to  $1 \times 10^8 \text{ cm}^{-3}$  with radio-frequency (rf) powers of 0.005–2 W, and lock-in times of 0.3–1.2 sec, under varying plasma and antenna conditions. It should be noted that the largest signals can be seen directly on a spectrum analyzer without using a lock-in. An interesting feature of this scattering system is that it can be continuously driven during a measurement across the outer minor radius of the plasma at constant scattering angle. A Princeton Applied Research 5202 50-MHz bandwidth lock-in allows direct interferometry (in the rf sense) of the IBW signal. Phase information, obtained here without varying plasma parameters,<sup>1</sup> is contained in the oscillating heterodyne photocurrent  $I_B$ :

$$I_B \propto \tilde{n} \exp[-(k_{\perp} - k_B)^2 a_0^2 / 8] \cos(k_{\perp} x_0),$$

for  $k_{\perp} \approx k_B$ , where  $k_B$  is the wave vector satisfying

the Bragg scattering condition,  $x_0$  is in the direction of the major radius, and  $\tilde{n}$  is the amplitude of the fluctuating component of the electron density at the pump frequency with perpendicular wave number  $k_{\perp}$ . By scanning  $x_0$ , a very accurate measurement of  $k_{\perp}$  similar to probe interferometry in the case of a long-wave train, as in Fig. 2(a), can be obtained. In Fig. 2(b) we show a comparison of a twin tip microcoaxial floating probe signal (tips  $\parallel B$ ) with the laser heterodyne photocurrent at a 12.3-MHz IBW frequency. Good agreement is obtained between the dispersion relation measured by the probe and laser.

Radial ion-temperature profiles, independent of knowledge of  $T_e$  or  $n_e$ , can be readily obtained through measurement of the local IBW perpendicular wavelength. In Fig. 3(a) we show calculated curves of  $\lambda_{\perp}$  versus radius  $r$  at different ion temperatures (using an independently measured abundance of  $H_1^+ \sim 50 \pm 5\%$ ,<sup>12</sup> remainder being  $H_2^+$ ,  $H_3^+$  at this fill pressure) and data points from a single laser waveform at  $f = 12.4 \text{ MHz}$  ( $\leq 0.5\text{-W}$  rf power). Then in Fig. 3(b) we plot  $T_i$  vs  $r$  at two hydrogen neutral fill pressures, as seen by laser and probe.

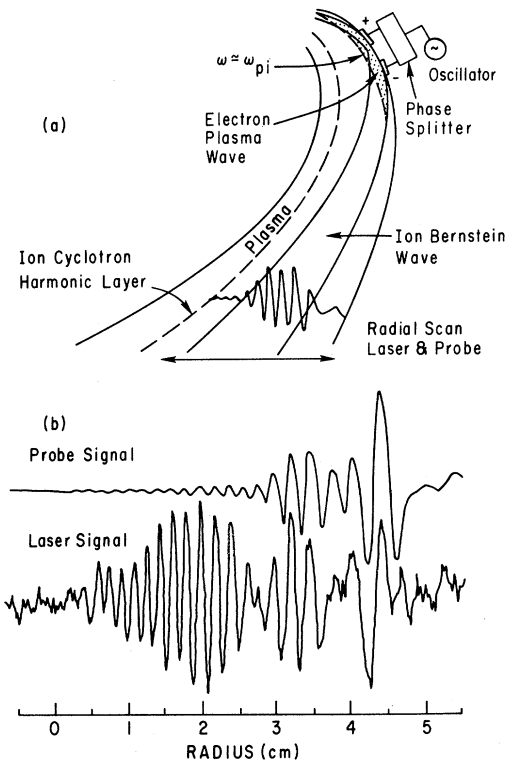


FIG. 2. (a) Schematic of IBW propagation, launched from external electrostatic plate antennas. (b) Comparison of detected IBW perpendicular waveforms at  $f = 12.3 \text{ MHz}$ , 1.8 W rf, neutral fill pressure  $P = 4 \times 10^{15} \text{ Torr}$ . The antennas are at  $r = 6.5 \text{ cm}$ .

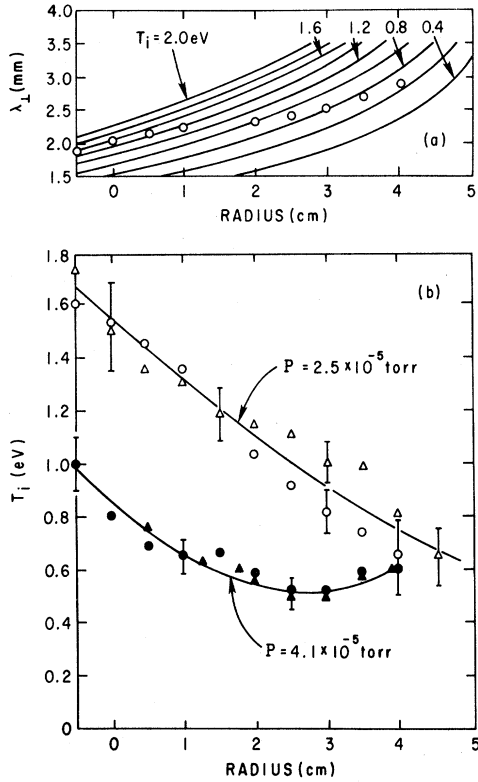


FIG. 3. Radial hydrogen ion temperature determination. (a) Computer generated constant  $T_i$  curves, and measured laser points at  $f = 12.4$  MHz,  $N_{H_1^+} = 50\%$ ,  $P = 2.5 \times 10^{-5}$  Torr,  $\lambda_{\parallel} = 34$  cm,  $T_e = 2$  eV,  $n_{e0} = 3.5 \times 10^{10}$  cm $^{-3}$ . (b) Comparison of radial temperature profiles obtained by laser (circles) and probe (triangles) from single frequency waveforms, at two neutral fill pressures.

Central ion temperature is observed to scale approximately inversely with neutral fill pressure.

We have run an independent Fabry-Perot ion temperature measurement with a mixed argon-hydrogen plasma. At a measured 20% H $^+$  concentration, a simultaneous comparison between the argon bulk ion energy, as inferred from the full width half maximum Doppler linewidth of the  $\pi$  component of singlet Ar II 4806 Å averaged along a central vertical chord, and the IBW derived hydrogen ion temperature, showed agreement to within 10%.

Higher harmonic IBW in pure hydrogen can also be observed, both of the major ion species H $_1^+$ , and of H $_2^+$ , H $_3^+$ . These three species effectively model H $^+$ , D $^+$ , T $^+$  with regard to resonances in the IBW dispersion relation. In Fig. 4, using internal grid excitation, we see a more complete portion of the IBW dispersion relation, showing up to the fourth harmonic of H $_1^+$  [Fig. 4(a)], and clear indications of the eighth harmonic of H $_3^+$  [Fig. 4(b)]. Laser data are

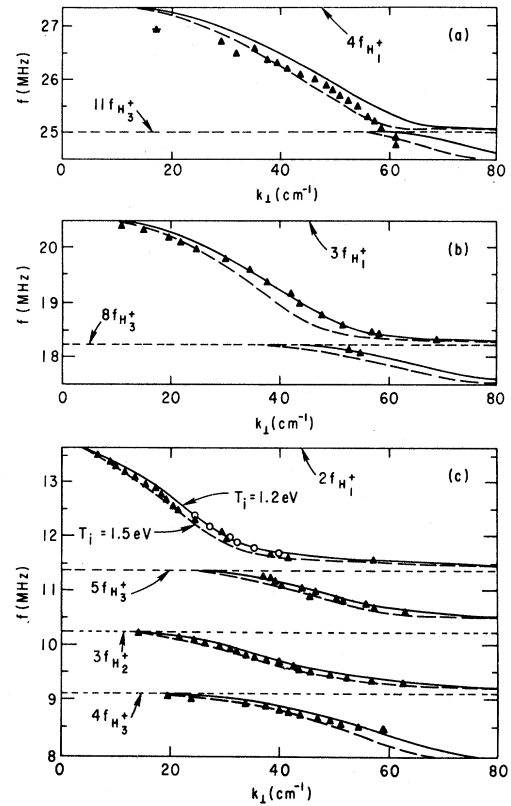


FIG. 4. Ion Bernstein wave dispersion relation, hydrogen plasma. Laser points (O), probe points ( $\blacktriangle$ ), using internal grid excitation. Data taken at  $r = 1.5$  cm,  $n_e = 2.4 \times 10^{10}$  cm $^{-3}$ ,  $P = 2.5 \times 10^{-5}$  Torr,  $\Omega_{H_1^+}/2\pi = 6.83$  MHz,  $T_e = 2$  eV,  $\lambda_{\parallel} \sim 130$  cm. Theoretical curves at two  $T_i$  values bracket data points. (a) Fourth-harmonic IBW branch of H $_1^+$ . (b) Third harmonic of H $_1^+$ , and evidence of eighth of H $_3^+$ . (c) Second-harmonic IBW branch used for  $T_i$ , and lower-frequency branches for H $_2^+$ , H $_3^+$  concentrations.

limited at small wave numbers by the small scattering angle, and at large wave numbers by wave front curvature, resulting in poor signal-to-noise ratios associated with low absolute fluctuation levels in this plasma. The effects of a multispecies plasma are evident in Fig. 4(c). Here the theoretical curves give a best fit H $_1^+$ :H $_2^+$ :H $_3^+$  in ratio  $50 \pm 3 : 28 \pm 2 : 22 \pm 2$ , in agreement with independent  $N_i$  measurements, yielding one ion temperature  $T_i = 1.35 \pm 0.2$  eV for all three species, as expected from estimated ion equilibrium times  $\leq 50$   $\mu$ sec. The second-harmonic IBW of H $_1^+$  and lower-frequency branches are particularly insensitive to  $n_e$  and  $k_{\parallel}$  and allow a good determination of  $T_i$  and relative concentrations.

In a typical tokamak, the ion temperature is higher by  $\sim 10^3$ , the toroidal  $B$  field by  $\sim 10^1$ , and  $f$  by  $10^1$ , so that using Eq. (2) we see that  $\lambda_1$  of interest is in

the range of 0.2–2 cm, suitable for far-infrared or 1-mm microwave scattering techniques. From the standpoint of wave physics, we observe that the relevant parameter for comparison to this work is  $k_{\perp} V_T / \Omega_i \sim 0.1-2$ , the same in ACT-1 as in a tokamak. Wave accessibility and poloidal field effects have been investigated, and should pose no insurmountable problems.<sup>14</sup>

In summary, we have successfully measured radial hydrogen ion temperature profiles independent of  $n_e$ ,  $k_{\parallel}$ , and  $T_e$ , using laser scattering to determine the perpendicular wavelength of an externally excited ion

Bernstein test wave. We believe a variation of this technique, taking into account possible difficulties inherent in a tokamak measurement, may show promise as a new  $T_i$  diagnostic.

The authors would like to thank C. M. Surko and R. E. Slusher for valuable advice early on in the scattering setup, E. Tolnas for help with the Fabry-Perot, and J. Taylor and W. Kineyko for their invaluable technical support. This work was supported by the U.S. DOE under Contract No. DE-AC02-76-CHO3073.

<sup>1</sup>C. M. Surko, R. E. Slusher, D. R. Moler, and M. Porkolab, Phys. Rev. Lett. **29**, 81 (1972).

<sup>2</sup>D. R. Baker, N. R. Heckenberg, and J. Meyer, Phys. Lett. **51A**, 185 (1975).

<sup>3</sup>H. Park, W. A. Peebles, A. Mase, N. C. Luhmann, Jr., and A. Semet, Appl. Phys. Lett. **37**, 279 (1980).

<sup>4</sup>C. M. Surko, R. E. Slusher, and J. J. Schuss *et al.*, Phys. Rev. Lett. **43**, 1016 (1979).

<sup>5</sup>E. Holzhauer, Phys. Lett. **62A**, 495 (1977).

<sup>6</sup>A. Gondhalekar and F. Keilmann, Opt. Commun. **14**, 263 (1975).

<sup>7</sup>E. R. Ault and H. Ikezi, Phys. Fluids **13**, 2874 (1970).

<sup>8</sup>J. P. M. Schmitt and T. Lehner, Phys. Rev. Lett. **45**,

1185 (1980).

<sup>9</sup>T. Tsukishima, Jpn. J. Appl. Phys. **19**, L534 (1980).

<sup>10</sup>M. Ono and K. L. Wong, Phys. Rev. Lett. **45**, 1105 (1980).

<sup>11</sup>C. Christopoulos and P. J. Christiansen, Plasma Phys. **16**, 499 (1974).

<sup>12</sup>M. Ono, K. L. Wong, and G. A. Wurden, Princeton Plasma Physics Laboratory Report No. 1819 (unpublished).

<sup>13</sup>R. E. Slusher and C. M. Surko, Phys. Fluids **23**, 3 (1980).

<sup>14</sup>M. Ono *et al.*, in *Proceedings of the Second Joint Grenoble-Varenna International Symposium on Heating in Toroidal Plasmas, Como, Italy, September, 1980*, edited by G. G. Leotta (Commission of European Communities, Brussels, 1981), Vol. 1, p. 593.